Open Archive Toulouse Archive Ouverte (OATAO)

OATAO is an open access repository that collects the work of Toulouse researchers and makes it freely available over the web where possible.

This is an author-deposited version published in: http://oatao.univ-toulouse.fr/
Eprints ID: 8982

To cite this version:

Msolli, Sabeur and Baazaoui, Ahlem and Dalverny, Olivier and Alexis, Joël and Karama, Moussa *Viscoplastic behavior of diamond die attach subjected to high temperature conditions.* (2012) In: 13th International Conference on Thermal, Mechanical and Multi-Physics Simulation and Experiments in Microelectronics and Microsystems, EuroSimE 2012, 16-18 Apr 2012, Lisbon, Portugal.

Any correspondence concerning this service should be sent to the repository administrator: staff-oatao@listes-diff.inp-toulouse.fr

Viscoplastic behavior of diamond die attach subjected to high temperature conditions

S. MSOLLI, A. BAAZAOUI, O. DALVERNY, J. ALEXIS, M. KARAMA

Université de Toulouse ; INP/ENIT ; LGP ; 47, avenue d'Azereix ; F-65013 Tarbes, France

smsolli@enit.fr, ahlem.baazaoui@enit.fr, olivier.dalverny@enit.fr, joel.alexis@enit.fr, Moussa@enit.fr

Abstract

In power electronic applications, diamond based semi-conductors appears to be a new way to widely increase the capabilities of power electronic converters [1, 2]. The main prospective expected is an increasing in system integration and power capabilities. The Diamonix project concerns the elaboration of a single-crystal diamond substrate with electronic quality and its associated packaging. The designed structure has to resist to temperatures varying between -50°C and +300°C. This paper deals with an experimental and numerical study of the diamond die attach solution. The development of a packaging for diamond component relies in particular on a specific choice of solder's alloys for the junction die/substrate. To carry out this junction, AuGe and AlSi eutectic alloys were chosen and characterized; the choice of these two kinds of solders i.e. AuGe and AlSi is motivated by the practical elaboration process and the restrictions of hazardous substances (RoHS). The first solder has a melting temperature of 356°C; the second has a higher melting point of 577°C. In this paper, we present some numerical results obtained from FE simulations of two 2D configurations of simplified electronic packaging. The power electronic packaging is composed of a diamond die and a copper metallized Si_3N_4 ceramic substrate which are brazed together with either AuGe or AlSi solder alloy. To predict the thermomechanical behavior of the solders, a particular constitutive behavior law was implemented as a User MATerial subroutine which is based on a viscoplastic unified McDowell formulation, coupled with porous damage equations. The mechanical law can describe precisely the viscoplastic damage phenomenon of solder subjected to high thermal cycling and to optimize the thermo-mechanical modeling for advanced package development.

1. Experimental characterizations of solders

For temperatures of about 300°C, the solder materials exhibit viscoplastic mechanical behavior. In order to identify the dependency on temperature and strain rates for the two solders, a set of experimental results, such as simple shear, creep and cycling tests are realized at 25, 200 and 300°C using specific shear specimens [3]. The specimens are mounted into a material testing machine equipped with a thermal enclosure for test temperatures up to 300°C. For creep tests, applied forces vary between 100 and 250 N. The database obtained is used for identification of material parameters of the viscoplastic damage model [4, 5]. We used finite element model for the lifetime prediction of the packaging under thermal or power cycling. The obtained results in 2D and 3D basic packaging configurations allow us to prepare for a design of experiment (DOE) of the diamond die packaging to find the optimal geometrical configuration for the new diamond packaging.

2. Experimental results analysis

In Fig. 1, we present some results from creep, simple and cyclic shear tests for the two solders.
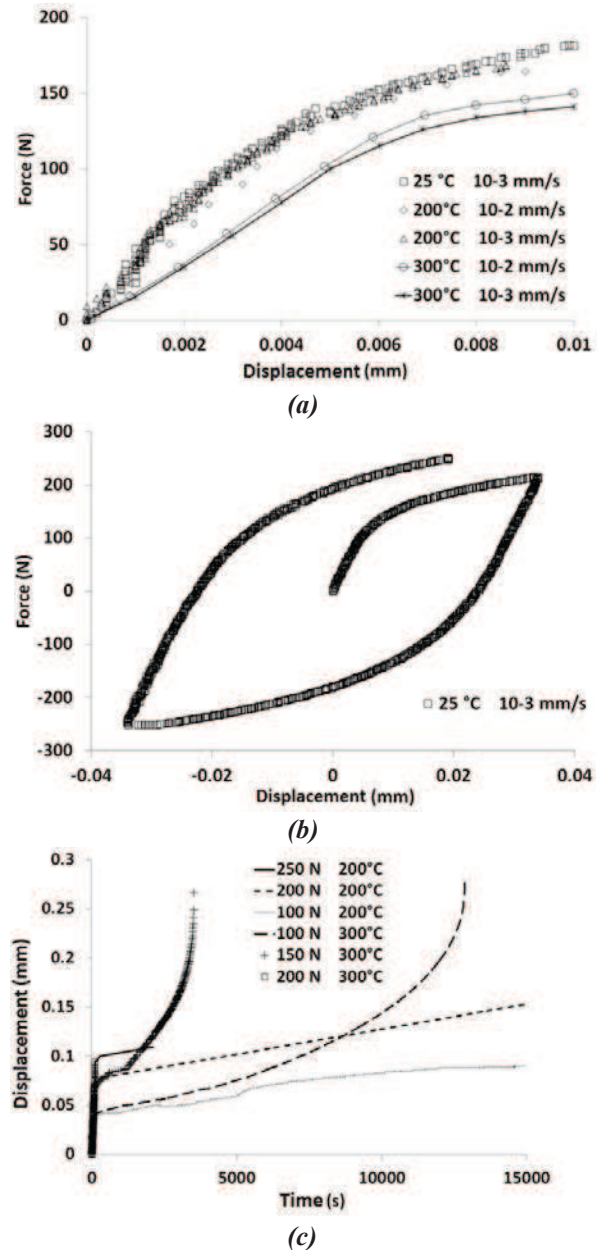

(a)

(b)

(c)

Figure 1: Results of realized mechanical tests using AuGe shear specimen, (a) simple shear, (b) cyclic shear, (c) creep.

In the case of AuGe solder, Fig. 1(a) shows the results of shear tests realized at various temperatures and displacement rates. The maximal applied force does not exceed 200 N whatever the imposed temperature. See that AuGe shows more sensitivity to strain rate at temperature of 300°C. This is due to the activated viscous mechanisms in the microstructural level such as dislocation climb and dislocation glide. Fig. 1(b) also demonstrates that AuGe solder exhibit cyclic hardening and Bauschinger effects due to shear.

Fig .1(c) represents the creep behavior of AuGe solder at various temperatures and loads. At 300°C, effect of creep is preponderant. Failure produces fast for the chosen forces 100 N, 150 N and 200 N.
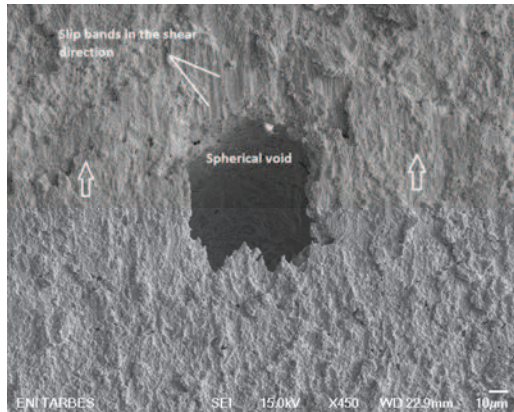

Figure 2: Micrographs of AuGe specimen failure profiles: initial voids fraction due to reflow process.

Fig. 2 shows specimen failure profiles after simple shear loading at 200°C and a displacement rate of 6.10^{-2} mm/min. The failure profiles are heterogeneous but show that deformation hardening produces in the shear direction. However, we can notice the presence of an initial voids fraction with spherical form. These voids have an average diameter of 100 µm. The presence of voids is essentially due to the solder reflow process during specimen manufacturing and have to be optimized to reduce their volumic fraction.
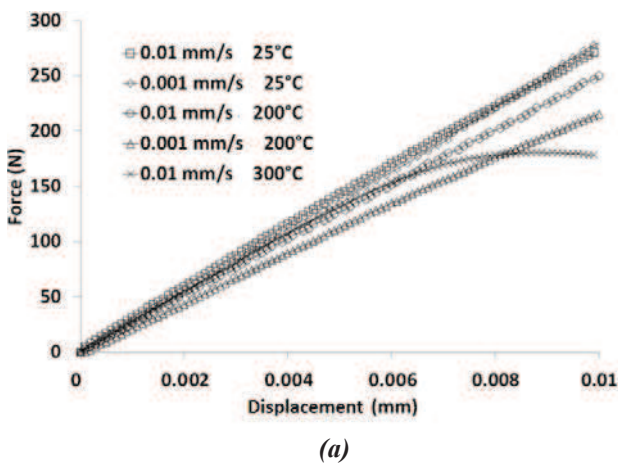
(a)
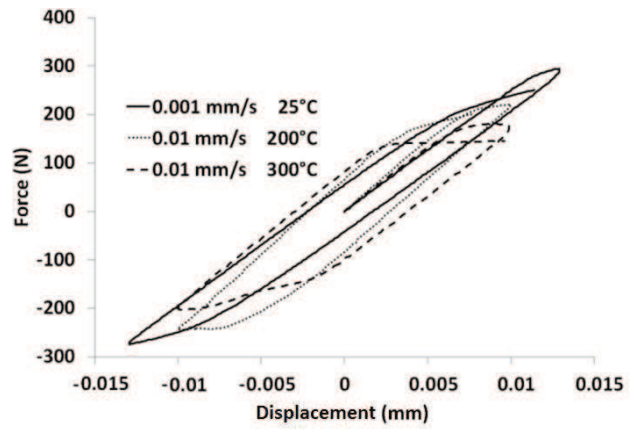
(b)

Figure 3: Results of realized mechanical tests using AlSi shear specimen, (a) simple shear, (b) cyclic shear.

Mechanical behavior of AlSi solder alloy is presented in Fig 3. For the simple shear tests, AlSi solder demonstrates a weak sensitivity to displacement rate even at high temperature. Moreover, it was mainly elastic behavior for temperatures up to 200°C and the applied forces reach a high value of 300 N. At 300°C, the yield stress decreases and plasticity is reached (Fig. 3(a)). A fast saturation level is reached due to the high material ductility. The AlSi mechanical behavior stills very close to Aluminium hardening behavior. In the cyclic case, there is also a weak amount of plasticity either for a temperature of 200°C. Contrarily to AuGe mechanical behavior, there is no Bauschinger effect for the AlSi solder but the material shows cyclic softening for the first cycle whatever the displacement and temperatures imposed. This softening behavior is combined to force saturation (200 N) at 300°C.
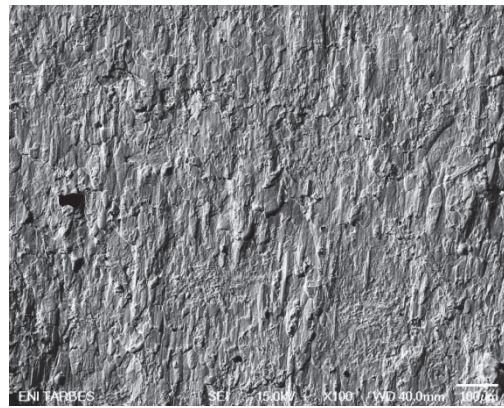

Figure 4: Micrographs of AlSi specimen failure profiles: shear bands in the load direction.

Fig. 4 illustrates the failure profile of the AlSi specimen. There are small shear bands oriented to the load direction. This bands show high ductility of AlSi material and prove that failure produces on the solder volume. There is no apparent voids present in the solder layer after the reflow process of the solder.

3. Modeling and damage prediction of 2D simplified packaging architecture

The simplified structure of a 2D power electronics packaging is showed is Fig 5(a). A half model is considered in this study. The packaging consists on a diamond die brazed to a Copper metallized Si_3N_4 ceramic substrate using a solder layer which can be either AuGe or AlSi. The packaging is subjected to thermal cycling decomposed into two steps: the first step consists on the reflow cycle included in the manufacturing process. The second step is the thermal cycling imposed for a temperature range of -50°C to 300°C with a temperature ramp of 20°C/min. There is a hold period of 30 min at both 300°C and -50°C. The whole thermal cycle is illustrated in the Fig. 5(b).
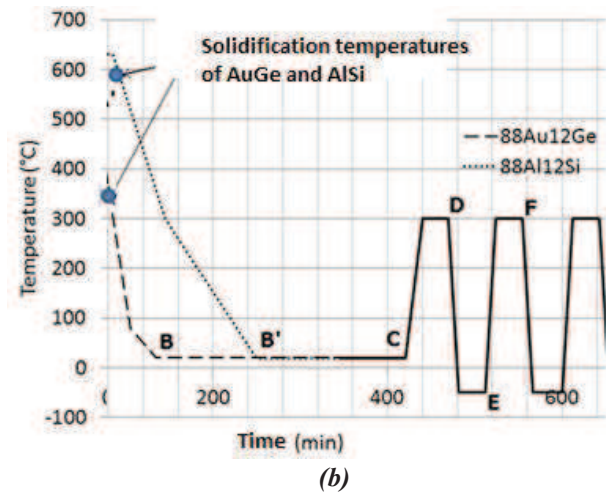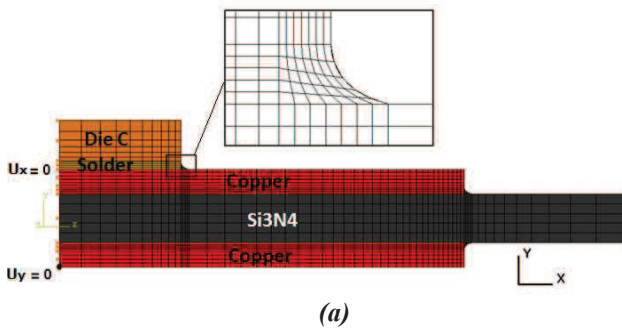

(a)

(b)

Figure 5: Modeling of 2D power electronics packaging, (a) simplified packaging architecture, (b) imposed temperature profile.

The diamond and Si_3N_4 ceramic are taken as pure elastic materials. Copper metallization is considered to have elastoplastic mechanical behavior with combined hardening. The die attach exhibit viscoplastic behavior which follows the coupled viscoplastic McDowell law and potential based damage rules. The model is integrated using a semi-implicit Euler scheme combined with a line search strategy [6]. The complete model parameters are identified using simple shear and creep experimental data. Damage parameters are identified using cyclic data giving maximal force versus number of cycles. Note that no interfacial behavior is considered between solder and die

deposits. There is no consideration of the effects of intermetallic compounds which implies that failure produce purely in solder layers. Only voids nucleation and growth are taken into account in the damage model [7]. Coalescence of voids is not considered in the modeling.

Simulations are conducted using the finite element code Abaqus®. The stress and strain values are extracted on the solder layer for comparison purposes between the two solder solutions. Damage profiles produced for 10 thermal cycles are plotted and compared for the two packaging configurations.
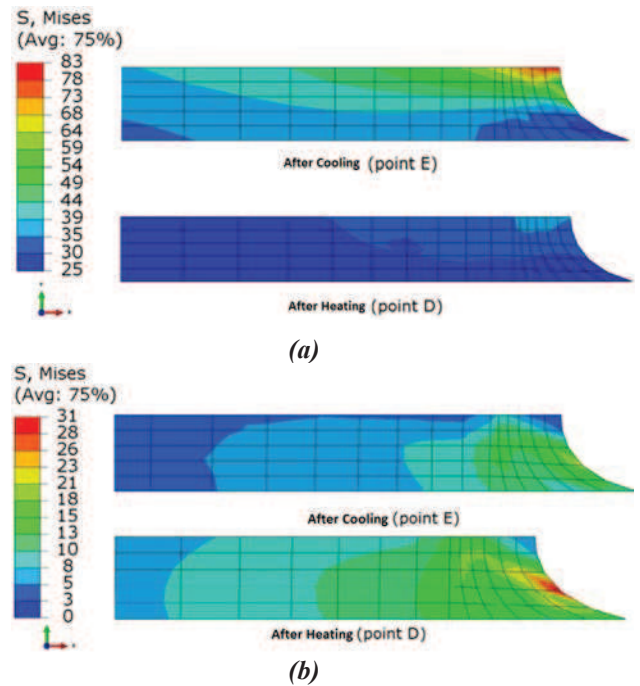

(a)

(b)

Figure 6: Stress distribution in the solder layers after thermal cycling of the two configurations, (a) AuGe, (b) AlSi.

Fig. 6(a) shows the stress distribution on the AuGe solder layer after heating and cooling. Stress is higher in the cooling step near the interface between die and solder. This is obvious because diamond has the highest rigidity among the whole assembly materials. The solder is more solicited in the die side and hardens during cycling. The effective stress reaches a value of 83 MPa. Note that AuGe behavior is monitored by combined kinematic-isotropic hardening behavior.

In the other hand, AlSi solder shows much less hardening in such way that the maximal stress in the solder is concentrated on the middle of the layer fillet. The value of the effective stress is about 30 MPa at the heating stage of the thermal cycling (Fig. 6(b)). AlSi behavior presents many similarities to Aluminium because it describes pure isotropic hardening and a stabilization of stress at advanced stage of loading.
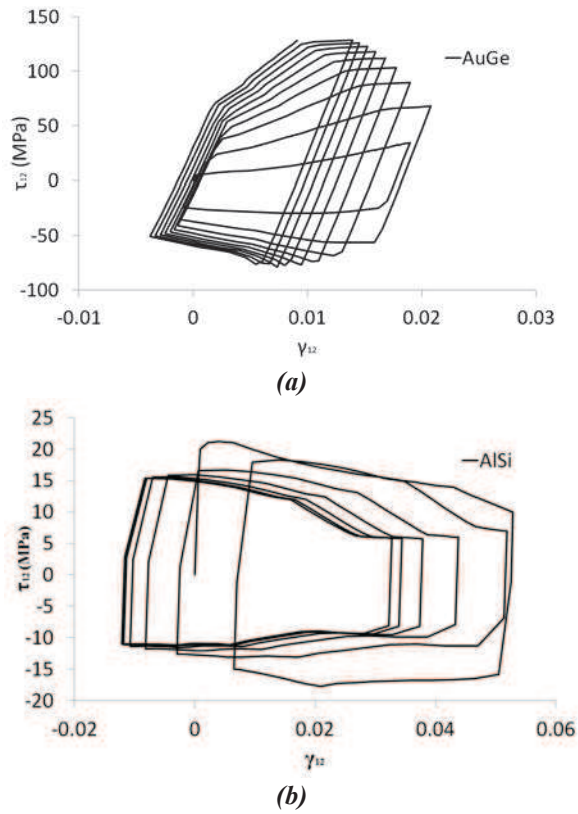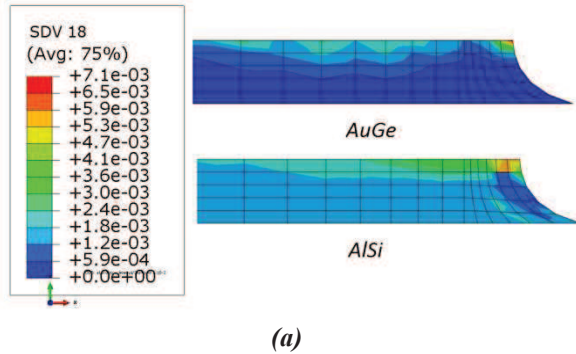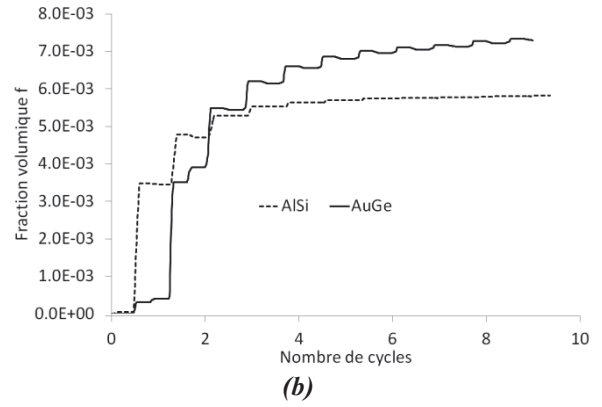
(a)

(b)

Figure 8: Evaluation of damage in the two solder layers, (a) FE results of damage distribution, (b) damage variation with respect to number of cycles for the two solders.

Looking at the damage profile in Fig. 8, we see that in the case of AuGe-based assembly, damage tends to be stable at the end of loading and takes a maximal value of 7.4E-3 in the solder layer. This amount of damage is higher than that observed in the AlSi solder layer which stabilizes at 5.7E-3 for a total number of thermal cycles equal to 10. Thus, for high thermal loading, AlSi seems to accumulate much less damage than AuGe. That is obvious because AlSi is subjected to cyclic softening and the stress produced in the solder still less important than that produced in AuGe solder. Regarding the evolution of damage in the two solders, we can conclude that the AlSi based packaging, represents a quite good prospective for high temperature high power applications in comparison with AuGe based assemblies.

4. 3D Modeling and damage prediction of AlSi based test vehicle

A 3D power electronics test vehicle was designed for thermal and power cycling. The vehicle is disposed as a "sandwich" structure and consists on diamond die brazed using AlSi solder alloy on Mo metallized Si_3N_4 ceramic substrate. The distance between the two vehicle halves are controlled using a molybdenum guide brazed to the die and the Mo metallization. The molybdenum guide is used to minimize the breakdown voltage risk and as a link between the two packaging parts.

(b)

Figure 7: Hysteresis loops at the end of the thermal cycling.

Hysteresis loops representing shear stress versus shear strain are extracted at an integration point of the layer where shear stress is maximal. These responses illustrated in Fig. 7 demonstrate the hardening characters of the two solders. In fact, for the AuGe solder, shear stress increases from 25 to 130 MPa and stabilizes at this value at the end of the cycling stage (Fig. 7(a)). The total shear strain reaches 2.5% at the first cycle of loading then it decreases progressively to 1.5% at the end of loading. However, for AlSi solder, there is a stress softening decreasing the stress from 22 MPa to 15 MPa and the stress response stabilizes in the 7th cycle. The shear strain is more important than AuGe shear strain and increases from 4% to a value of about 6%. Then the two solders show completely opposite mechanical behaviors and are expected to describe different damage profiles.
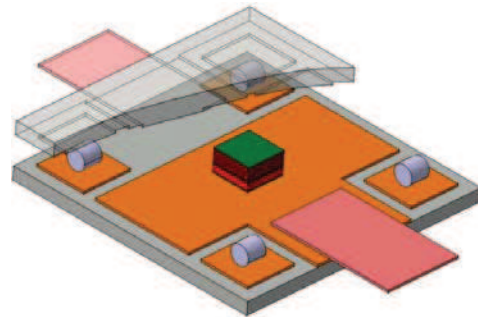

(a)

Figure 9: 3D geometric configuration of the power electronics test vehicle.

Four cylindrical Molybdenum bumps are brazed to the Mo metallization for mechanical support of the system. Thus, AlSi solder is used for both die/Mo, and Mo/Mo assemblies. Two connection leads in Molybdenum ensure electrical power conduction. The test vehicle is subjected to the same thermal cycling illustrated in Fig. 5(b). The composition of the 3D vehicle test is detailed in Fig. 9.
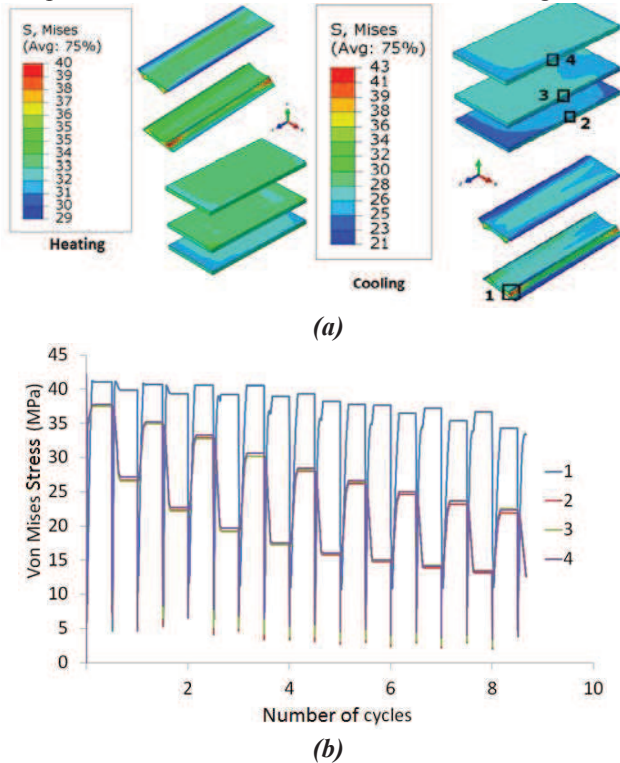

(a)

(b)

Figure 10: Evaluation of stress in the solder layers, (a) FE results of stress distribution, (b) stress variation with respect to number of cycles in various solder regions.

Fig. 10 shows the difference of stress amplitudes in the various regions of solder layers (denoted 1,2,3 and 4 in Fig. 10(a)). Following this figure, stress in the bumps solders (1 in Fig. 10(a)) are much more important than the other regions stress. It takes a value of 40 MPa in the first heating stage and a maximal value of 43 MPa in the first cooling stage. The other stress profiles still the same degrading stress from 37 MPa tending to a stable value of 20 MPa.
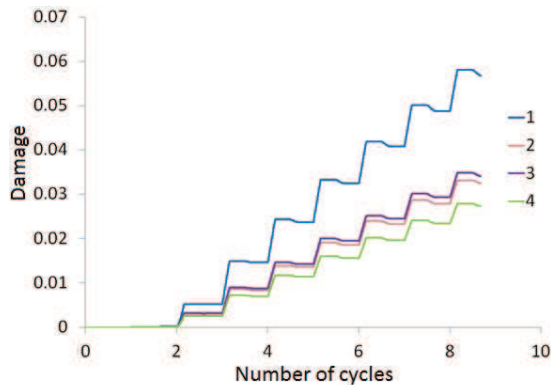

Figure 11: Progression of damage in four solder regions of the test vehicle.

For all cases, stress softening is viewable in all regions.

Concerning damage evolution, Fig. 11 illustrates damage profiles in the four regions. As expected, damage in the bumps solder is nearly twice higher than the other values and keeps increasing until 6% at the 10th cycle. For the damage, stabilization (essentially due to voids nucleation) is not reached and may take many computations efforts. But a conservative prediction consists on assuming a continuous linear evolution of damage and extrapolating the damage profiles to determine the numbers of cycles N_f which permit to have a volumic fraction of damage of 50%. This limit is fixed by the "Standard Military Handbook" and represents the criteria for the packaging validity [8].

Following this method, the failure is expected to start in bumps solders after a minimum period of about 62 cycles (1 in Fig(10(a)), in Die/Mo solder layers (2 and 3 in Fig. 10(a)) after 110 cycles and in Mo/Mo solder layers (4 in Fig. 10(a)) after 130 cycles.

4. Conclusions

Two diamond-based packaging configurations designed for high temperature and high power applications are studied. The packaging are composed with two kinds of high temperatures solders AuGe and AlSi. The experimental data permitted to approve the viscoplastic mechanical behavior of the two solder alloys and gives a database to identify the material parameters for a coupled porous damage and viscoplastic model. The last is used for the FE modeling of 2D and 3D packaging architecture. The FE modeling permitted to demonstrate that AlSi based packaging represents a good prospective for extreme temperature power electronics applications. The model shows that failure may happen in the bumps solders for the 3D test vehicle which must be proved experimentally. Studies of the test vehicle under power cycling must be explored to identify and evaluate failure.

References

1. Brezeanu, M., *et Al*, "On-state behaviour of diamond Schottky diodes" *Diamond & Related Materials*, Vol. 17, (2008), pp.717-740.
2. Lostetter, A.B., *et Al,* "An overview to integrated power module design for high power electronics packaging" *Microelectronics Reliability,* Vol. 40, (2000), pp.365-379.
3. Msolli, S., *et Al*, "Mechanical characterization of an Au-Ge solder alloy for high temperature electronic devices" *Proc 6th Integrated Power Electronics Systems Conf*, Nurmeberg, GER, Marsh. 2010, pp.1-5.
4. Fu, C., *et Al*, "Time Integration Procedures For A Cyclic Thermoviscoplasticity Model for Pb-Sn Solder Applications" *Proc 46th Electronic Components and Technology Conf*, Orlando, FL, May. 1996, pp. 403-413.
5. Haghi, M. and Anand, L., "A constitutive model for isotropic, porous, elastic-viscoplastic metals" *Mechanics of Metals*, Vol. 13, No.1, (1992), pp.37-53.

6. Msolli, S., *et Al*, "Implicit integration scheme for porous viscoplastic potential-based constitutive equations" *Procedia Engineering*, Vol. 10, (2011), pp. 1544-1549.

7. Gurson, A. L., "Plastic Flow and Fracture Behaviour of Ductile Materials Incorporating Void Nucleation, Growth And Coalescence" PhD Dissertation, Brown University, 1975.

8. Military Standard Handbook , MIL-STD-883G 2030.